ISSN 1674-1056
http://cpb.iphy.ac.cn
http://iopscience.iop.org/cpb
中国物理 B
Chinese Physics
中国物理
Chinese Physics B

A 37 mJ, 100 Hz, high energy single frequency oscillator

Yu Shen(申玉), Yong Bo(薄勇), Nan Zong(宗楠), Shenjin Zhang(张申金), Qinjun Peng(彭钦军), and Zuyan Xu(许祖彦)

Citation: Chin. Phys. B, 2021, 30 (**8**): 084208. DOI: 10.1088/1674-1056/ac0694
Journal homepage: http://cpb.iphy.ac.cn; http://iopscience.iop.org/cpb

What follows is a list of articles you may be interested in

Effect of thermally induced birefringence on high power picosecond azimuthal polarization Nd:YAG laser system

Hongpan Peng(彭红攀), Ce Yang(杨策), Shang Lu(卢尚), Ning Ma(马宁), Meng Chen(陈檬)
Chin. Phys. B, 2019, 28 (**2**): 024205. DOI: 10.1088/1674-1056/28/2/024205

Linear polarization output performance of Nd: YAG laser at 946 nm considering the energy-transfer upconversion

Jin-Xia Feng(冯晋霞), Yuan-Ji Li(李渊骥), Kuan-Shou Zhang(张宽收)
Chin. Phys. B, 2018, 27 (**7**): 074211. DOI: 10.1088/1674-1056/27/7/074211

Development of an injection-seeded single-frequency laser by using the phase modulated technique

Shu-Tao Dai(戴殊韬), Hong-Chun Wu(吴鸿春), Fei Shi(史斐), Jing Deng(邓晶), Yan Ge(葛燕), Wen Weng(翁文), Wen-Xiong Lin(林文雄)
Chin. Phys. B, 2018, 27 (**5**): 054212. DOI: 10.1088/1674-1056/27/5/054212

Random lasing in dye-doped polymer dispersed liquid crystal film

Rina Wu(乌日娜), Rui-xin Shi(史瑞新), Xiaojiao Wu(郜小娇), Jie Wu(吴杰), Qin Dai(岱钦)
Chin. Phys. B, 2016, 25 (**9**): 094209. DOI: 10.1088/1674-1056/25/9/094209

Experimental study of electro-optical *Q*-switched pulsed Nd:YAG laser

A Maleki, M Kavosh Tehrani, H Saghafifar, M H Moghtader Dindarlu
Chin. Phys. B, 2016, 25 (**3**): 034206. DOI: 10.1088/1674-1056/25/3/034206

A 37 mJ, 100 Hz, high energy single frequency oscillator*

Yu Shen(申玉)[1,2,†], Yong Bo(薄勇)[1,2], Nan Zong(宗楠)[1,2], Shenjin Zhang(张申金)[1,2,‡], Qinjun Peng(彭钦军)[1,2], and Zuyan Xu(许祖彦)[1,2]

[1] *Research Center for Laser Physics and Technology, Technical Institute of Physics and Chemistry, Chinese Academy of Sciences, Beijing* 100190, *China*
[2] *Key Laboratory of Solid State Laser, Key Laboratory of Function Crystal and Laser Technology, Chinese Academy of Sciences, Beijing* 100190, *China*

(Received 2 May 2021; revised manuscript received 27 May 2021; accepted manuscript online 29 May 2021)

Ways on energy enhancement for single frequency oscillator are reported in this paper. By quantitative analysis on gain and loss coefficients for each cavity mode with inserted etalons, a 37 mJ, 100 Hz high energy single-frequency Nd:YAG oscillator is obtained. The pulse energy is promoted by enhancement of nearly 7 times for a single frequency oscillator reported. The result proves that this method does help for energy enhancement. It has attractive potential for high energy single frequency oscillator design, especially on condition of intensive side pumped or long cavity laser, where strong competitors exist and are hard to be suppressed.

Keywords: Nd:YAG laser, high pulse energy, single frequency oscillator

PACS: 42.55.–f, 42.60.–V, 42.60.Da **DOI:** 10.1088/1674-1056/ac0694

1. Introduction

Single-frequency Nd:YAG laser has a wide range of applications, as optical metrology, high-resolution spectroscopy, coherent detection,[1–8] and especially Fourier-telescopy (FT).[9–18] To obtain a single-frequency laser, three problems need to be solved, including single longitudinal mode selection, single transverse mode selection, and energy enhancement. For single longitudinal mode selection, several ways have been developed, such as short cavity configuration,[19–23] microchip lasers,[23,24] non-planar ring oscillator,[25–30] traveling-wave cavity,[31–39] twisting mode lasers, and inserted multi etalons.[31–42] Techniques used for single transverse mode selection include inserted aperture or lens, long cavity, end pump laser, and thermally near unstable resonator.[31–43] For energy enhancement, a master-oscillator power-amplifier is a well-established technique.[44–52] Isyanova reported a 55 mJ single-frequency laser by a MOPA system, and the oscillator has the energy of 0.8 mJ with inserted etalon.[47] Tong reported 101 mJ single-longitudinal-mode Nd:YAG laser by a pre-amplifier and amplifier system and the oscillator has an energy of 1.25 mJ obtained by a short cavity with inserted etalon.[48] A 500 mW nonplanar ring oscillator (NPRO) was amplified to 800 mJ/pulse by an injection seeded oscillator and four slab amplifiers system.[49] A 10 mJ single frequency pulse was realized by an injection seeded oscillator, and amplified to 200 mJ.[50] Liem reported 100-W single-frequency radiation by the use of a MOPA system,[30] with near 63 times of amplifying ability. NASA Langley research center has developed a 100 mJ/pulse single-frequency laser, using an injection seeded ring oscillator.[5,12] Northrop Grumman demonstrated a 15 kW CW single-frequency MOPA system,[2,51] the oscillator was low-power with less than 200. Xu *et al.* reported a 700 mJ pulse energy single-frequency 1064 nm laser by using seed injection and a three-stage MOPA system. Xu *et al.* reported a 700 mJ pulse energy single-frequency 1064 nm laser by using seed injection and a three-stage MOPA system. The 10 mW single-frequency CW oscillator is amplified to 0.7 W by a fiber amplifier and to 350 W (700 mJ/pulse) by the MOPA system, it is a powerful amplifier with amplifying ability of $3.4 \subseteq 10^4$ times.[52] The MOPA investigation shows attractive potential for energy/power scaling and it makes the principal validation viable. The problem is that the MOPA system is too complex and huge for application, as the pulse energy of oscillators is limited to several milli-Joule levels now. It helps for a further breakthrough that energy enhancement of the oscillators to dozens of milli-Joule level, but it is rarely reported. As conflict lies in energy enhancement and fixing it at a single frequency synchronously.

Ways on energy enhancement for single frequency oscillator is reported in this paper. By quantitative analysis on gain and loss coefficients for each cavity mode with inserted etalons, a 37 mJ, 100 Hz high energy Nd:YAG single frequency oscillator is experimentally obtained. It is designed and obtained by a side pumped three-mirror annular cavity with inserted etalons. This configuration increases the injected pump energy, compared with the traditional end-pumped short cavity. And it introduces a number of strong competitors as

*Project supported by the National Natural Science Foundation of China (Grant No. 11504389) and the Funds of Key Lab of Function Crystal and Laser Technology, Technical Institute of Physics and Chemistry, Chinese Academy of Sciences.

†Corresponding author. E-mail: shenyu@mail.ipc.ac.cn
‡Corresponding author. E-mail: zhangshenjin@mail.ipc.ac.cn

© 2021 Chinese Physical Society and IOP Publishing Ltd

well, including transverse and longitudinal modes. Longitudinal mode selection with multi etalons is a well-established technique, it has great potential for high energy oscillator design but limited to be 5.5 mJ now. How to select a single mode out by the inserted multi etalon, from strong competitors, is investigated theoretically and experimentally.

2. Quantitative analysis on the single mode selection

Side pumped configuration offers perfect pump energy storage ability, and it is a potential choice for energy scaling of single-frequency laser, but has not been used as yet. The bottleneck is that two problems appear and need to be solved. The first one is that as the input energy increases, the laser gain and thermal effect enhance, which introduces longitudinal or transverse multimode oscillation and stability deterioration. The second one is that to offer enough suppression for transverse mode, the longer cavity length is preferred, which increases the numbers of longitudinal modes and sets a challenge on longitudinal mode selection. The two problems are quantitatively analyzed in this section, including single longitudinal mode operation and stability control, and single transverse mode operation and stability control from large numbers of strong competitors under the extremely high gain.

2.1. Single longitudinal mode selection and stability control

Single longitudinal mode selection and stability control are theoretically analyzed. For Nd:YAG laser, the line profiles follow a Lorentz function $f(\nu)$ as follows:

$$f(\nu)=\frac{\Delta\nu_{\rm cry}/2\pi}{(\nu-\nu_0)^2+\left(\Delta\nu_{\rm cry}/2\right)^2}, \tag{1}$$

$$\Delta\nu_{\rm q}=\frac{c_0}{2nL_{\rm cavity}}, \tag{2}$$

where $\Delta\nu_{\rm cry}$ is the line width of the Nd:YAG crystal, and ν_0 is the frequency at the center of the homogeneously broadened linewidth. The number of longitudinal modes oscillated in the cavity is determined by the homogeneously broadened line width of the Nd:YAG crystal $\Delta\nu_{\rm cry}$ and the frequency spacing of two adjacent longitudinal modes in the cavity $\Delta\nu_{\rm q}$. When the cavity length of the oscillator is 30 mm, 15 longitudinal modes oscillate in the cavity. As the cavity length of the oscillator enlarges to 950 mm, 500 longitudinal modes may appear. Selecting 1 from the 500 longitudinal modes and fixing it for a long time, instead of 1 from tens of modes, is the first challenge. It means making a high gain for the 1 needed and a high loss for all the 499 artificially. To meet this challenge, the laser oscillation is theoretically analyzed and simulated, including the gain and loss coefficient for each cavity mode. It gives quantitative analysis on the parameter design and optimization of the etalons.

Laser gain for each frequency is given by

$$G(\nu)=\frac{G^0(\nu)}{1+\frac{I(\nu)}{I_{\rm s}}\frac{f(\nu)}{f(\nu_0)}}, \tag{3}$$

$$G^0(\nu)=\Delta n^0 B_{21}\frac{\mu}{c}h\nu_0 f(\nu), \tag{4}$$

$$B_{21}=\frac{c^3}{8\pi h\nu^3\mu^3\tau_{\rm f}}, \tag{5}$$

where $G^0(\nu)$ is the small-signal gain coefficient, $I(\nu)$ is the power density in the system for each frequency, $I_{\rm s}$ is the saturation flux, B_{21} is the simulated radiation coefficient, μ is the refractive index, and $\tau_{\rm f}$ is the lifetime for spontaneous radiation of the upper laser level. Δn^0 is the maximum value of population inversion. The number of ions for the excited upper laser level, the lower laser level, and the ground state are n_2, n_1, and n_0, respectively.

The change rate of the electron population densities for the two laser levels in a four-level laser system is analyzed by the following equations:

$$\frac{{\rm d}n_2}{{\rm d}t}=W_{\rm P}n_0-\left(n_2-\frac{g_2}{g_1}n_1\right)\sigma\phi c-\frac{n_2}{\tau_{\rm f}}, \tag{6}$$

$$\frac{{\rm d}n_1}{{\rm d}t}=\left(n_2-\frac{g_2}{g_1}n_1\right)\sigma\phi c+\frac{n_2}{\tau_{21}}-\frac{n_1}{\tau_{10}}, \tag{7}$$

$$\frac{{\rm d}\phi_1}{{\rm d}t}=c\phi\sigma n-\frac{\phi}{\tau_{\rm c}}, \tag{8}$$

$$n_{\rm tot}=n_1+n_2+n_0, \tag{9}$$

$$n_2=n_0W_{\rm p}\tau_{\rm f}, \tag{10}$$

$$n_0W_{\rm p}=n_{\rm Q}\eta_{\rm s}P_{\rm ab}/(h\nu V), \tag{11}$$

$$\Delta n_0=\tau_{\rm f}n_{\rm Q}\eta_{\rm s}P_{\rm ab}/(h\nu V), \tag{12}$$

where $W_{\rm p}$ is the pumping rate (s^{-1}), ϕ is the photon density (photons/cm^3), $n_{\rm tot}$ is the total number of atoms is the two levels, g_1, g_2 are degeneracies of the two energy levels, $c=c_0/n$ is the velocity of light in the laser medium, σ is the cross-section for the stimulated emission, $\tau_{\rm c}$ is the decay time of photon in the cavity, $\tau_{\rm f}$ is the fluorescence decay time of the upper laser level, τ_{21} is the lifetime for spontaneous radiation of level E_2, and τ_{10} is the lifetime for radiation of level E_1, in an ideal four-level system the terminal level empties infinitely fast to the ground level $\tau_{10}\approx 0$. Form Eqs. (6)–(11), the maximum number of ions for upper laser level E_2 is deduced. In an ideal four-level system $n_1=0$ and $\Delta n^0=n_2$, then the maximum value of population inversion Δn^0 is obtained by Eq. (12), where $\eta_{\rm Q}$ is the quantum efficiency, $\eta_{\rm B}$ is the overlapping efficiency, and $\eta_{\rm s}$ is the Stokes factor.

Laser gain of the system for each frequency is deduced by Eqs. (3) and (12)

$$G(\nu)=\frac{\tau_{\mathrm{f}}\eta_{\mathrm{Q}}\eta_{\mathrm{s}}c^2}{16h\pi^3r^2L\mu^2\tau_{\mathrm{f}}}\cdot\frac{\eta_{\mathrm{abs}}P_{\mathrm{pump}}}{f\tau_{\mathrm{p}}}\cdot\frac{\left(\Delta\nu_{\mathrm{cry}}/2\right)^2}{(\nu-\nu_0)^2+\dfrac{2\eta_{\mathrm{Q}}\eta_{\mathrm{s}}\eta_{\mathrm{B}}}{(L_{\mathrm{loss}}-InR_{\mathrm{oc}})\,\pi r^2}\dfrac{\sigma\tau_{\mathrm{f}}}{h\nu}\dfrac{\eta_{\mathrm{abs}}P_{\mathrm{pump}}}{f\tau_{\mathrm{p}}}\left(\Delta\nu_{\mathrm{cry}}/2\right)^2}$$
$$\times\frac{\nu_0\Delta\nu_{\mathrm{cry}}}{\nu^4\left[(\nu-\nu_0)^2+\left(\Delta\nu_{\mathrm{cry}}/2\right)^2\right]},\tag{13}$$

where Stokes factor $\eta_{\mathrm{s}}=\lambda_{\mathrm{p}}/\lambda_{\mathrm{L}}$, L is the crystal length, r is the crystal radius, P_{pump} is the pump power, η_{abs} is the absorption efficiency, f is the repetition rate, τ_{p} is the pulse duration, R_{oc} is the reflectivity of the output coupler, and L_{loss} is the loss coefficient of the cavity.

The oscillation condition for a laser system with multi mirrors and multi etalons is

$$\mathrm{e}^{2[G(\nu)-\alpha]L}R_1R_2\cdots R_{\mathrm{i}}T_{\mathrm{FP1}}(\nu)\,T_{\mathrm{FP2}}(\nu)\cdots T_{\mathrm{FP}j}(\nu)=1,\tag{14}$$

where α is the laser crystal loss coefficient, R_i is the reflectivity for each mirror, and $T_{\mathrm{FP}j}(\nu)$ is the transmittance for each etalon at different frequencies described by

$$T_{\mathrm{FP}j}(\nu)==\frac{1}{1+\frac{4r}{(1-r_j)}\sin^2\frac{2\pi}{c}n_jd_j(\nu-\nu_0)\cos\theta}.\tag{15}$$

Here r_j is the reflectivity and d_j is the thickness of etalons numbered as 1 to j. There is no analytical solution for multi etalons design. To give a numerical solution, the oscillation condition is changed to be

$$G(\nu)=\alpha-\frac{1}{2L}\mathrm{In}\left[R_1R_2\cdots R_{\mathrm{i}}T_{\mathrm{FP1}}(\nu)\,T_{\mathrm{FP2}}(\nu)\cdots T_{\mathrm{FP}j}(\nu)\right].\tag{16}$$

The right part of the above equation is denoted as the loss coefficient of each cavity mode for convenience,

$$\alpha(\nu)=\alpha-\frac{1}{2L}\mathrm{In}\left[R_1R_2\cdots R_{\mathrm{i}}T_{\mathrm{FP1}}(\nu)\,T_{\mathrm{FP2}}(\nu)\cdots T_{\mathrm{FP}j}(\nu)\right].\tag{17}$$

The laser gain and loss coefficients of the system for each cavity mode are quantitatively described by Eqs. (13) and (17). Two solid F–P etalons are selected for the simulation in this paper, one is employed as a main etalon (r_1, d_1), having high fineness selectivity for unwanted longitudinal modes suppression; the other is employed as assistor (r_2, d_2), having a large free spectral range for unwanted longitudinal modes suppression. Parameters used in the simulation are summarized in Table 1, and the result is illustrated in Fig. 1. When the pump power is designed to be 240 W with 100 Hz repetition rate and 200 microseconds pulse duration, the optimized working parameters of the main etalon and the assistor are (90%, 6 mm) and (70%, 0.7 mm), respectively. On this condition, the frequency spacing of two adjacent longitudinal modes in the cavity is $\Delta\nu_{\mathrm{q}}=368$ MHz, the 6 mm main etalon has a free spectral range of $\Delta\nu_1=17$ GHz, inducing a 62 % loss for the adjacent longitudinal modes besides, as shown in Fig. 2; it is sufficient to eliminate neighboring axial cavity modes oscillation. The 0.7 mm assistant etalon has a free spectral range of $\Delta\nu_2=148$ GHz, inducing 80 % loss for the adjacent strongest longitudinal mode of the main etalon, ±17 GHz from the center, thus the possibility of laser oscillations at this mode and other similar resonances is suppressed. Two adjacent transmission peaks of the assistant etalon appear at ±148 GHz away from the center, but have small influence, as they are close to the edge of 150 GHz gain line shape which falls off sufficiently to prevent laser oscillation at such frequencies. The gain coefficient for the aimed frequency is designed to be between two values, one is the loss coefficient of the aimed frequency and the other is the loss coefficient of the strongest competitors. This design ensures a stable operation under operation fluctuation.

Table 1. Parameters used in the simulation.

Parameters	Value
Planck constant h	6.26×10^{-34} J·s
Refractive index of Nd:YAG crystal μ	1.82
Crystal length L	80 mm
Crystal radius r	1 mm
Loss coefficient of Nd:YAG crystal α	0.001 cm^{-1}
Fluorescence decay time τ_{f}	230×10^{-6} s
Stimulated cross section of Nd:YAG crystal σ	6.5×10^{-19} cm^2
Linewidth of Nd:YAG crystal $\Delta\nu_{\mathrm{cry}}$	150 GHz
Cavity length of the oscillator L_{cavity}	946.2 mm
Quantum efficiency η_{Q}	0.95
Overlapping efficiency η_{B}	0.95
Wavelength of pump laser λ_{p}	808 nm
Wavelength of excited laser λ_{L}	1064 nm
Pump power P_{pump}	240 W
Absorption efficiency η_{abs}	0.8
Repetition rate f	100 Hz
Pulse duration τ_{P}	200 μs
Loss coefficient of the cavity L_{loss}	0.1

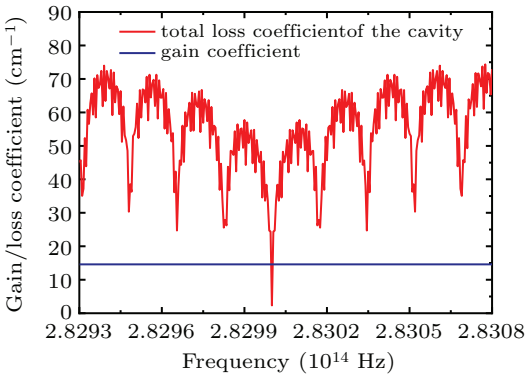


Fig. 1. Laser gain and loss coefficient for each cavity mode with two etalons.

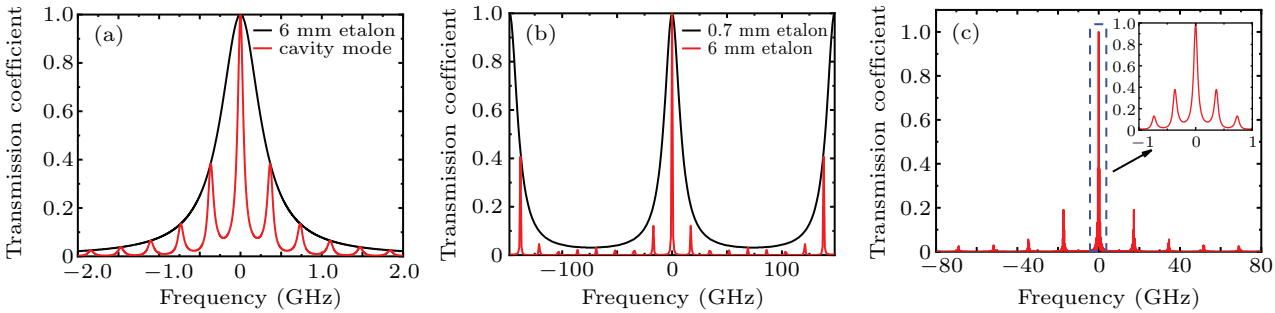


Fig. 2. Multimode oscillation suppression of the main etalon (a), the assistant etalon (b), and the total effect (c).

2.2. Single transverse mode selection and stability control

The second problem that needs to be solved is single transverse mode operation and stability control under high laser gain operation. To reduce the high order oscillation of transverse mode, a thermally near unstable resonator with inserted aperture is designed. Under the thermally near-unstable condition, the laser operates at the border of the stable region, where the fundamental model size is larger and the diffraction loss for the high-order is higher, so high output power and good beam quality can be expected.

To enhance the output energy and reduce laser oscillation loss, the aperture size and its location are simulated, measured, and modified quantitatively. The simulated value of fundamental mode size distribution $\omega_{\text{simu}}(Z)$ is obtained at a given working thermal lens, cavity length, and curvature of cavity mirrors.[50] On working condition of the laser cavity, the beam characteristics of the laser output is measured by a beam quality analyzer (M2-200, Spiricon Inc.), recorded as $\omega_{\text{simu}}(Z)$. The spatial distribution of the laser beam at the output coupler or inside the oscillator is deduced according to the ABCD matrix of Gaussian beam's propagation and transmission physics in free space or optical element. The simulated and measured value at the same location will modify the simulation parameters and give instruction on the location and diameter design of the inserted quartz diaphragm on condition of $\omega_{\text{simu}}(Z) = \omega_{\text{seas}}(Z)$.

3. Experimental investigation

A high pulse energy 1064 nm single frequency oscillator is experimentally constructed. The arrangement is illustrated in Fig. 3. The side pumped resonant cavity is built up by three mirrors, flat mirrors M1, M2, and 55.6° polarizer P. Two identical laser heads LH1 and LH2 are diode-side-pumped, to enhance the storage ability of pump power and realize a high energy output. Each laser head contains three-dimensional bar arrays, four lines on each dimension, with a total pump power of 240 W, the wavelength of 808 nm. The laser gain medium used in this experiment is Nd:YAG crystal cylindrical rods provided by Cryslaser Inc. A 90° quartz rotator is placed between the two laser heads to compensate for the thermally induced birefringence. The unidirectional operation of the ring laser is enforced by a combination of a Faraday rotator (FR), a half-wave plate (HW), and together with a 55.6° polarizer ($R = 99\%$ for S polarization, $R = 5\%$ for P polarization). The Nd:YAG rod is 80 mm in length and 2 mm in diameter, 1 at.% doped, polished, and anti-coated at end faces. All intracavity elements are antireflection coated at 1064 nm, except for the two etalons. The optical length of the cavity is 946.2 mm.

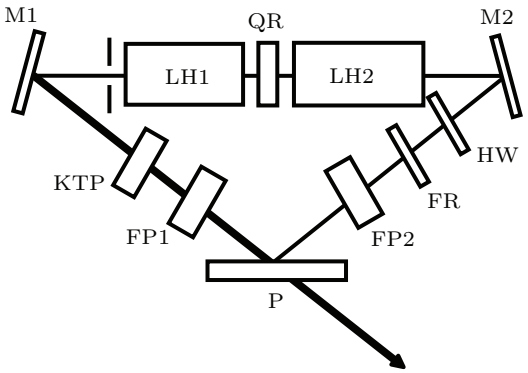


Fig. 3. Schematic of the single frequency laser. QR: 90° quartz polarization rotator, LH1, LH2: diode-side-pumped laser head, FR: Faraday rotator, P: thin film polarizer, HW: half-wavelength wave plate, M1, M2: reflective mirrors (17.2°, $R > 99.8\%$).

Without transverse mode selection element, the oscillator shows a multimode oscillation mode with an un-centralized energy distribution, with a beam quality of 3.41 in the x-direction and 3.7 in the y-direction, as shown in Fig. 4(a). As the thermal focusing effect is not severe at low repetition frequency of 100 Hz, it fails to realize high power with good beam quality by the thermally near unstable cavity design. Instead, a quartz aperture is inserted to select the TEM_{00} mode out, and its diameter and location are further optimized experimentally under the simulated value. The separation degree between the TEM_{00} mode and the higher orders gives influence on the selectivity of the aperture. When it has a suitable size at the favorite location, a stable near diffraction limited beam quality is obtained under power fluctuation. The optimized size is 1 mm in diameter, and the optimized location is 160 mm away from the reflective mirrors M1/M2, on two arms. The beam quality is then enhanced by 18% after optimization, to

be 1.26 in the x-direction and 1.32 in the y-direction measured by Spiricon M2-200, compared in Fig. 4(b).

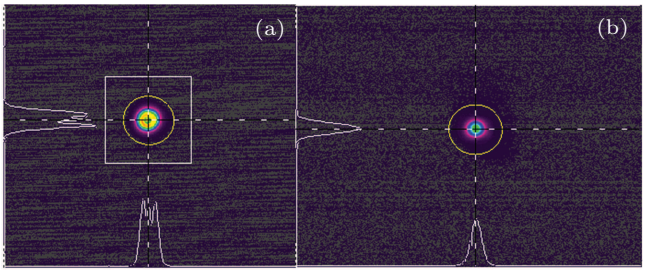


Fig. 4. Beam quality of the cavity without (a) and with (b) inserted aperture.

The optimized double F–P etalon is used to obtain stable single axial mode operation. The F–P etalons are thermally tuned to select a single axial mode near the center of the gain curve and tilted to decouple them from each other. The double F–P etalon mode filter gives a sufficient reduction in transmission so that any other mode is below the threshold at a cost of 42% laser power loss.

The laser spiking caused by periodic pumping and relaxation oscillation is harmful for application and it is suppressed by a non-linear crystal, KTP, to generate almost a rectangular laser pulse. The $5\times5\times5$ mm^3 KTP crystal converts high-intensity laser spikes into the second harmonic radiation, resulting in a reduction of the spike strength by 20%, and a reduction of relaxation time to 25%, then a smoother laser pluse is obtained, the suppression effect is shown in Fig. 5.

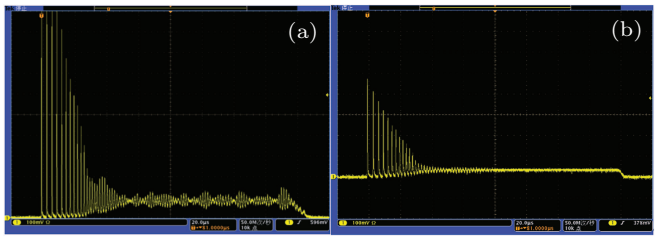


Fig. 5. The 1064 nm laser pulses without (a) and with (b) intracavity second harmonic generation.

By using the laser cavity designed and optimized above, the single-mode operation is obtained, with 37 mJ/pulse energy for a 200-microsecond duration pulse at 100 Hz repetition rate. The maximum fluctuation of laser power is less than 10% in 30 min (Fig. 6). The beam quality of the oscillator is 1.26 in x-direction and 1.32 in y-direction. The frequency bandwidth is less than 100 MHz, and the frequency fluctuation is less than 250 MHz, measured by WS-7, HighFinese GmbH. The measured frequency bandwidth and frequency fluctuation are both less than the 317 MHz frequency spacing of two adjacent longitudinal modes in the cavity, then the single-frequency operation is substantiated. The output energy shows no saturation trend, but the frequency fluctuation appears when the pump power continues to enhance. In addition, the time wavefront and the Fourier transformation of the spiking pulse are detected by an ultrafast photodiode and shown by an oscilloscope (Tektronix DPO 4104). The waveform is rather smooth, which shows no beat pattern of multiple longitudinal modes, the single frequency is further substantiated.

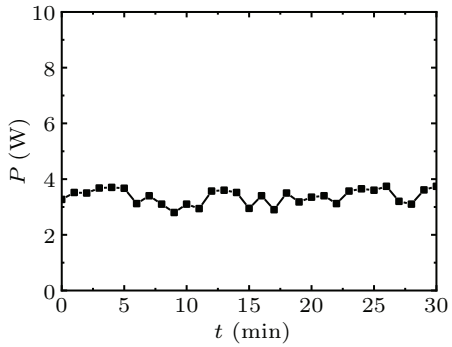


Fig. 6. Power stability of the oscillator in 30 min at the maximum average power.

4. Conclusions

A high-energy single frequency 1064 nm oscillator has been designed in this paper. For energy enhancement, a side pumped three-mirror annular cavity is designed and applied for single-frequency operation for the first time. This design has an advantage of favorite injecting and storage ability, compared with the end-pumped single-frequency lasers, and disadvantage of challenges in mode selectivity and control. Ways to select a single mode out with high precision from numbers of strong competitors by inserted multi etalon are investigated theoretically and experimentally. Then, a 37 mJ/pulse, 100 Hz repetition rate, 200-microsecond duration, near-diffraction-limited single-frequency laser is obtained. The line width of the longitudinal mode is less than 100 MHz, and the frequency fluctuation is less than 250 MHz. The single frequency oscillator reported in this paper promotes the single pulse energy by an enhancement of nearly 7 times for single pulse energy and more than 130 times for peak power compared with the single frequency seed laser developed by NASA. It makes pulse energy of up to >1 J/pulse possible by power amplification with a MOPA system.

References

[1] Ding Y Q, Qi Y F, Liu C, He J and Zhou J 2011 *International Symposium on Photoelectronic Detection and Imaging*, 19 August 2011, Beijing, China, 819220
[2] Redmond S, McNaught S, Zamel J, Iwaki L, Bammert S, Simpson R, Weiss S B, Szot J, Flegal B, Lee T, Komine H, Injeyan H and Ieee 2007 *Conference on Lasers and Electro-Optics*, 6–11 May 2007, Baltimore, Maryland United States, 2160
[3] Frank H K S, TObias M, Gerd M, Thomas S, Robert L, and Berry S 2004 *Proceedings of the 5th International Conference on Space Optics (ICSO 2004)*, 30 March–2 April 2004, Toulouse, France, 599
[4] Basu C, Wessels P, Neumann J and Kracht D 2012 *Opt. Lett.* **37** 2862
[5] Hovis F E, Edelman J, Schum T, Rudd J and Andes K 2008 *Recent progress on single frequency lasers for space and high altitude aircraft applications*, 14 February 2008, Bellingham E8710
[6] Peshko I I, Khiznyak A B, Dlugaszek A and Jabczynski J K 1996 *Tunable single-frequency diode-pumped Nd:crystal lasers for Doppler radar application*, 13 February 1996, Warsaw, Poland, 2729/31

[7] Dai S T, Jiang T, Wu L X, Wu H C and Lin W X 2019 *Acta. Phys. Sin.* **68** 134202 (in Chinese)
[8] Shen D, Ding L, Zhang Q, Zhu C, Wang Y, Zhang W and Zhang X 2020 *Chin. Phys. B* **29** ab8c41
[9] Aleksoff C C 1997 *Opt. Lett.* **1** 54
[10] Ustinov N, Anufriev A, Vol'Pov A, Zimin I and Tolmachev A 1987 *Soy. Quantum Electron* **17** 108
[11] Sica L 1992 *App. Opt.* **31** 120
[12] Prasad N, Singh U, Hovis F and Armstrong D 2006 *Proceedings of SPIE - The International Society for Optical Engineering*, 19 May 2006, Orlando (Kissimmee), Florida, United States, 27
[13] Cuellar E L, Stapp J and Cooper J 2005 *Laboratory and field experimental demonstration of a Fourier telescopy imaging system*, 23 August 2005, San Diego, California, United States, 58960D
[14] Mathis J, Stapp J, Cuellar E L, Cooper J, Morris A, Fairchild P, Hult D, Koski K, Ramzel L and Thornton M A 2005 *Optics and Photonics 2005*, 30 August 2005, San Diego, California, United States, 58960F
[15] Olsen R C 2007 *Remote sensing from air and space* (Bellingham, Washington: SPIE) 314
[16] Cuellar E L, Cooper J, Mathis J and Fairchild P 2008 *Laboratory demonstration of a multiple beam Fourier telescopy imaging system*, 26 August 2008, San Diego, California, United States, 70940G
[17] Spivey B, Stapp J and Sandler D 2006 *Phase closure and object reconstruction algorithm for Fourier telescopy applied to fast-moving targets*, 8 September 2006 San Diego, California, United States, 630702
[18] Stapp J, Spivey B, Chen L, Leon L, Hughes K, Sandler D and Cuellar E L 2006 *Simulation of a Fourier telescopy imaging system for objects in low Earth orbit*, 7 September 2006, San Diego, California, United States, 630701
[19] Danielmeyer H G 1970 *IEEE J. Quantum Electon.* **6** 101
[20] Agger S, Povlsen J and Varming P 2004 *Opt. Lett.* **29** 1503
[21] Lindberg H, Larsson A and Strassner M 2005 *Opt. Lett.* **30** 2260
[22] Shen D Y, Tam S C, Lam Y L and Kobayashi T 2000 *Opt. Rev.* **7** 451
[23] Wang Y, Huang L, Gong M, Zhang H, Lei M and He F 2007 *Laser Phys. Lett.* **4** 580
[24] Mooradian J J Z A A 1989 *Opt. Lett.* **14** 24
[25] Koch G J, Deyst J P and Storm M E 1993 *Opt. Lett.* **18** 1235
[26] Wu K Y, Yang S H and Wei G H 2002 *Opt. Commun.* **203** 323
[27] Kane T J and Byer R L 1985 *Opt. Lett.* **10** 65
[28] Bode M, Freitag I, Tünnermann A and Welling H 1997 *Opt. Lett.* **22** 1220
[29] Vance J D, She C Y and Moosmüller H 1998 *Appl. Opt.* **37** 4891
[30] Liem A, Limpert J, Zellmer H and Tünnermann A 2003 *Opt. Lett.* **28** 1537
[31] Kumar S C, Samanta G K, Devi K, Sanguinetti S and Ebrahim Z M 2012 *Appl. Opt.* **51** 15
[32] Clobes A R and Brienza M J 1972 *Appl. Phys. Lett.* **21** 265
[33] Dergachev A 2011 *Opt. Express* **19** 6797
[34] Johnston J T F, Brady R H and Proffitt W 1982 *Appl. Opt.* **21** 2307
[35] Jarrett S M and Young J F 1979 *Opt. Lett.* **4** 176
[36] Li M, Zhao W, Hou W, Zhang S, Guo L, Lin X and Li J 2012 *Appl. Phys. B* **106** 593
[37] Li M L, Zhao W F, Hou W, Xiong B, Zhang S B, Lin X C and Li J M 2011 *Laser Phys.* **21** 1738
[38] Martin K I, Clarkson W A and Hanna D C 1996 *Opt. Lett.* **21** 875
[39] Li M L, Zhao W F, Zhang S B, Guo L, Hou W, Li J M and Lin X C 2012 *Appl. Opt.* **51** 1241
[40] Cheng Y, Kringlebotn J T, Loh W H, Laming R I and Payne D N 1995 *Opt. Lett.* **20** 875
[41] Milovskii N V, Markelov N A and Il'in V A 1993 *Laser Phys.* **3** 821
[42] Rantamaki A, Rautiainen J, Sirbu A, Mereuta A, Kapon E and Okhotnikov O G 2013 *Opt. Express* **21** 2355
[43] Zeng X, Zhang M, Cao D, Sun D and Zhou H 2020 *Chin. Phys. B* **29** 064206
[44] Shuai L, Ya D G, Zhong Z C, Lin Z, Ke L G, Zhi F Z, Bao S W, Jian X, Yi T X, Lei Y, Yang K, Yang L, Yan Y L, Qin J P and Zu Y X 2019 *Chin. Phys. Lett.* **36** 044204
[45] Teng S, Jian G X and Yu C S 2019 *Chin. Phys. Lett.* **36** 034201
[46] Xue Z C, Pei L L, Zai Y W and Qiang L 2019 *Chin. Phys. Lett.* **36** 124201
[47] Urata Y, Kudo A, Wada S, Imai K and Ito 2003 *Quasi-CW laser diode pumped master-oscillator power-amplifier system in single frequency operation*, 22–27 June 2003, Munich, Germany, 77
[48] Tong L, Zhao Z, Cui L, Liu C, Chen J, Gao Q and Tang C 2011 *Laser Phys.* **21** 52
[49] Ma X, Wang J, Zhou J, Zhu X and Chen W 2011 *Appl. Phys. B* **103** 809
[50] Schröder T, Lemmerz C, Reitebuch O, Wirth M, Wührer C and Treichel R 2007 *Appl. Phys. B* **87** 437
[51] Goodno G, Komine H, McNaught S, Redmond S, William, Long, Simpson R, Cheung E, Howland D, Epp P, McGraw P, Weber M, McClellan M, Bell D, Serrano J, Sollee J, Injeyan H, Landers F and DaSilva H 2005 *Multi-kW near-diffraction-limited single-frequency Nd:YAG laser. Lasers and Electro-Optics Europe*, 12–17 June 2005, Munich, Germany, 25
[52] Xu X, Xie G, Lu Y, Zhang L and Wan M 2015 *High Power Laser Science and Engineering* **3** e24
[53] Baida L 2003 *Laser Optics* (Beijing: Higher Education Press) p. 235